

March · Vol. 84 · DP17644

# steel research

international

3  
2013

[www.steel-research.de](http://www.steel-research.de)

WILEY-VCH





# steel research

international



www.steel-research.de

## Cover Photo:

The cover shows a multifaceted parabolic solar concentrator and absorber at the Almeria Solar Platform, Spain, used to reduce hematite to magnetite. More details can be found in the manuscript by I. Ruiz-Bustanza et.al.

## Publishing company:

Wiley-VCH Verlag GmbH & Co. KGaA,  
Boschstraße 12, D-69469 Weinheim,  
Germany

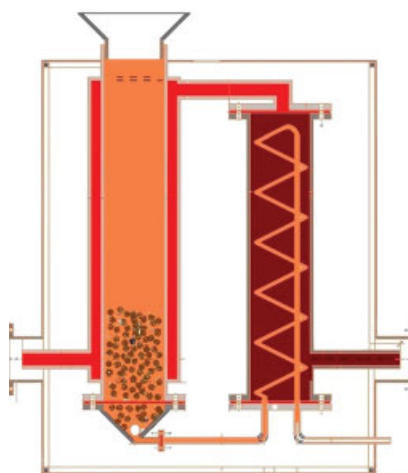
## Contents

### Full Paper

I. Ruiz-Bustanza\*, I. Cañadas,  
J. Rodríguez, J. Mochón, L. F. Verdeja,  
F. Garcia-Carcedo, and A. J. Vázquez

**Magnetite Production from Steel  
Wastes with Concentrated Solar  
Energy**

EDITOR'S CHOICE ————— 207



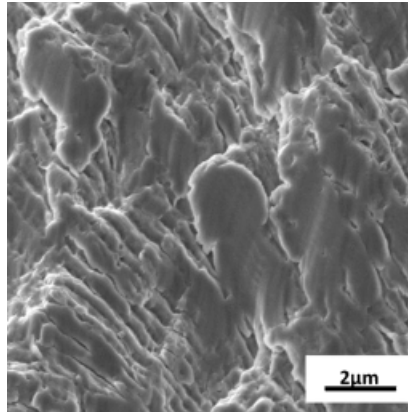
The use of solar thermal energy is quite interesting because of its direct application to metallurgical and chemical processes. A fluidized bed furnace, heated by solar energy has been used to reduce mill scale. The search of the objectives, “zero waste” and “clean energy”, may pose an interesting challenge in the manufacturing of primary iron and steel, as well as in areas of other metal production and even in the recycling of wastes, minimizing CO<sub>2</sub> emissions.

# Contents

T. S. Srivatsan\*, K. Manigandan, A. M. Freborg, and T. Quick

**Investigating and Understanding the Cyclic Fatigue, Deformation, and Fracture Behavior of a Novel High Strength Alloy Steel: Influence of Orientation**

218

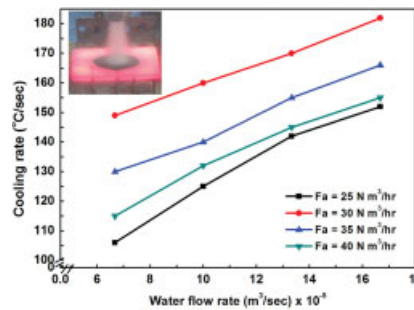


Influence of orientation on high cycle fatigue properties and final fracture behavior of alloy steel Pyrowear 53 is the focus. Test specimens prepared from both the longitudinal and transverse orientations were deformed in cyclic fatigue over a range of maximum stress, under fully-reversed loading, and number of cycles-to-failure recorded. The fracture surfaces were examined to establish the macroscopic mode and characterize intrinsic features on the surface.

S. S. Mohapatra, S. V. Ravikumar, S. K. Pal, and S. Chakraborty\*

**Ultra Fast Cooling of a Hot Steel Plate by Using High Mass Flux Air Atomized Spray**

229

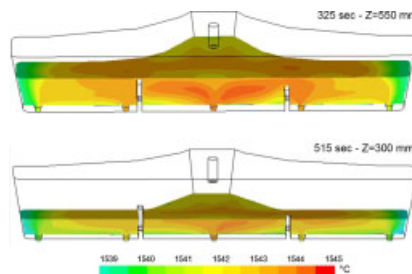


The ultra fast cooling of a 6 mm thick hot steel plate has been studied using high mass flux (>130 kgm<sup>-2</sup> s) air atomized spray. The heat transfer analysis depicts that air atomized spray has an excellent control over heat transfer even at a high initial surface temperature of 900°C and as a result the maximum cooling rate of 182°Cs<sup>-1</sup> has been achieved which is in the ultra fast cooling regime.

V. Battaglia, M. De Santis\*, V. Volponi, and M. Zanforlin

**Steel Thermo-Fluid-Dynamics at Tundish Drainage and Quality Features**

237



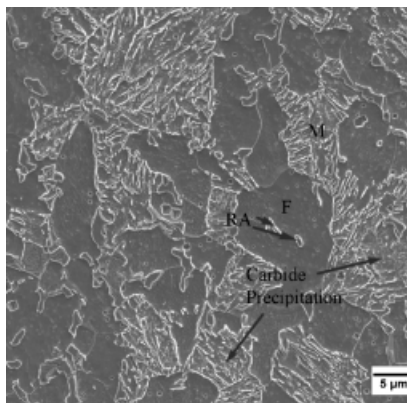
CFD modeling of steel flow and temperature fields are described during 5-strand long product tundish drainage at ORI Martin Steelworks. The vortices formation was shown, at first from the strands close to corners. The bath height was found to avoid slag entrapment through vortices. Once applied into operating practice, no rejection or claims for cleanliness were achieved. The beneficial effect of both good insulation and regular drainage rate to prevent steel freezing was found and confirmed by a ORI campaign at tundish start operations including about 700 heats.

# Contents

W. Feng\*, Z. Wu, L. Wang, and J. G. Speer

## Effect of Testing Temperature on Retained Austenite Stability of Cold Rolled CMnSi Steels Treated by Quenching and Partitioning Process

246

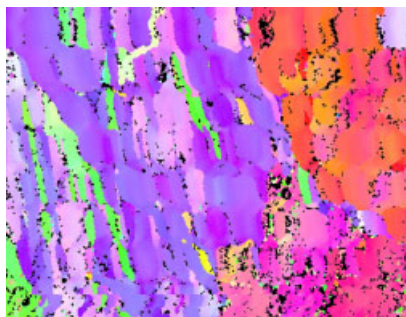


The effect of testing temperature on retained austenite stability of industrially cold rolled CMnSi sheet steel treated by quenching and partitioning process has been investigated through the deformation and transformation behavior of retained austenite at different testing temperatures. And a correlation between retained austenite stability and mechanical properties is also established.

J. J. Jonas\*, C. Ghosh, and V. V. Basabe

## Effect of Dynamic Transformation on the Mean Flow Stress

253

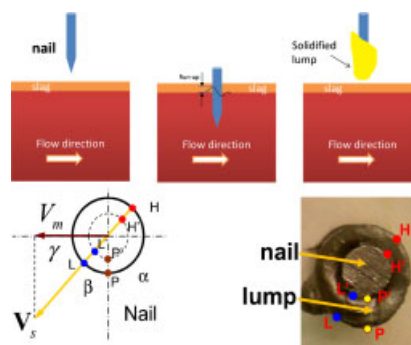


Mean flow stresses are calculated from experimental flow curves determined on four steels of increasing C content. These are plotted against inverse temperature so as to define the stress drop or upper critical temperature applicable to rolling. These temperatures are shown to be well above the equilibrium transformation temperatures, an observation that is attributed to the occurrence of dynamic transformation.

C. Ji\*, J. Li, H. Tang, and S. Yang

## Effect of EMBR on Flow in Slab Continuous Casting Mold and Evaluation Using Nail Dipping Measurement

259



The information provided in this paper can be applied in steel plant to measure the mold top surface velocity and meniscus fluctuation with time variation. This work can be used to investigate the effect of EMBR and others casting condition on mold surface flow pattern and furthermore improving the casting defect. Also the method in this paper provides a way to validate the accuracy of computational model. This paper is free of charge.

M. Raudensky\*, J. Horsky, J. Ondrouskova, and B. Vervaet

## Measurement of Thermal Load on Working Rolls during Hot Rolling

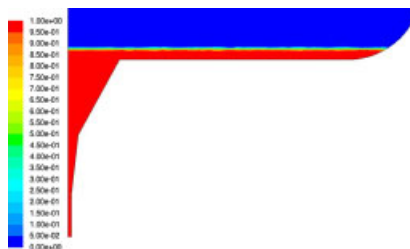
269



An experimental technique developed for monitoring the work roll surface temperature by sensors embedded in the work roll is presented. Continuous hot rolling pilot line trials were performed for different process conditions. These thermal measurements give very detailed information about the temperature field in the roll. The heat flux and heat transfer coefficient distribution along the roll circumference were obtained.

# Contents

P. Ni, L. T. I. Jonsson, and P. G. Jönsson\*  
**Simulations of the Ladle Teeming Process and Verification With Pilot Experiment**



Predicted interface in an inclined bottom ladle with an expanding diameter nozzle during teeming by VOF+ realizable  $k-\epsilon$  model with enhanced wall treatment.

276

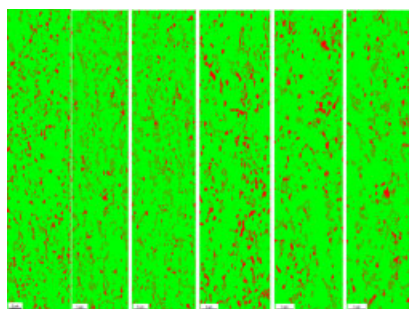
K. Janiszewski\*  
**The Slenderness Ratio of the Filter Used in the Process of Liquid Steel Filtration as the Additional Parameter of the Filter Form**



We propose in this publication the introduction of new, additional definition describing the multiple orifice ceramic filters used in research works on the liquid steel filtrations, calling this the filter slenderness ratio. Using this coefficient we obtain the possibility to compare the filtration effectiveness of different types of ceramic filters, not only for filters with cylindrical filtrating orifices, but also for other types, e.g., with orifices of rectangular section.

288

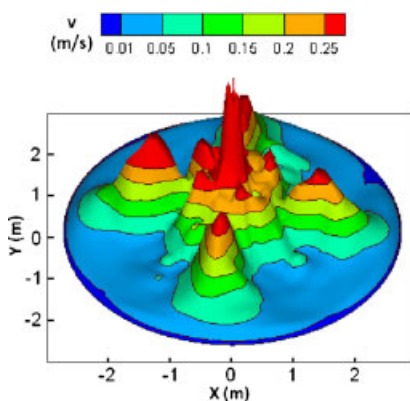
E. Emadoddin\*, A. Akbarzadeh, R. Petrov, and L. Zhao  
**Anisotropy of Retained Austenite Stability during Transformation to Martensite in a TRIP-Assisted Steel**



Strain induced martensitic transformation of retained austenite has been studied in Al-containing TRIP steel samples with similar retained austenite characteristics. It was found a difference of retained austenite stability by tensile straining along RD and TD. This behavior has been explained by the texture component of ferrite causes anisotropy of crystal plasticity so that more transformation of retained austenite is measured along RD rather than TD.

297

M. Lv\*, R. Zhu, H. Wang, and R. G. Bai  
**Simulation and Application of Swirl-Type Oxygen Lance in Vanadium Extraction Converter**



This paper described jet characteristics of conventional and various swirl-type oxygen lances by water model experiment and numerical simulation. The swirl-type oxygen lance was experimented in 150 t vanadium extraction converter. The research shows that the swirl-type lance can strengthen stirring ability and guarantee the normal converter vanadium extraction process. It is helpful to improve vanadium extraction efficiency.

304

# Magnetite Production from Steel Wastes with Concentrated Solar Energy

Iñigo Ruiz-Bustanza,\* Inmaculada Cañadas, Jose Rodríguez, Javier Mochón, Luis Felipe Verdeja, Fernando Garcia-Carcedo, and Alfonso J. Vázquez

In order to achieve a balanced development in the application of materials for structural or functional purposes, one of the priority objectives of future work is to achieve the goal of “zero waste” in the different production lines. As would be expected from what was agreed in the Kyoto Protocol and the meetings of Copenhagen 2009 and Cancun 2010, the production of clean energy will be strongly encouraged in the future, and indeed that is already the case now. Taking that into consideration, while the promotion of clean energy production is mainly directed toward electricity, solar thermal is quite interesting because of its direct application to metal mining and the chemical processes used in the sustainable development of materials. The combination of both objectives, “zero waste” and “clean energy,” may pose an interesting challenge in the development of primary iron and steel, as well as in other areas of metal production and even in the field of mining. The help of solar thermal energy, which can be concentrated to reach high temperatures, is a tool that could support both the direct production and the recycling of waste steel, in particular waste which is physically and chemically the worst for the environment. This would mean that the environment itself, solar energy, is in fact the key to environmental protection.

## 1. Introduction

The production of “clean energy” and the control of CO<sub>2</sub> emissions appear to be the most important parameters in new chemical processes and new material production in the next few decades. Approximately 4–5% of the CO<sub>2</sub> emissions of a given country are a result of metallurgical activity. However, in countries or regions with elevated integral or electrical steel production, the rate may reach as high as 10%.<sup>[1]</sup> Emissions attributed to the steel industry can range from 1.30 to 1.50 t of CO<sub>2</sub> per tonne of steel. Considering an annual world steel production of 1200 million tonnes, the CO<sub>2</sub> emitted by the steel industry can be as high as 1800 million tons per year.

Throughout the operations and processes for producing iron and steel are noticed what are well known as “metallurgical losses” and which are recorded to justify an efficiency of <100%. In most cases, this refers to products oxidized with varying amounts of carbon (reducing element) and non-ferrous metal oxides added through the ore or slag forming agents.

One particular “by-product,” known as mill scale, is generated in the process of austenitizing and the hot plastic deformation of steel (hot rolling). About 5 kg of mill scale is produced per ton of steel. The elementary iron composition is shown in **Table 1**.

In addition to the cost of installation, the reducer agent used and the energy consumed must also be taken into account when considering the bottom line for plants involved in recycling steel production wastes. The integration of solar thermal recycling processes would provide an eventual cost savings overall, as well as a source of a metallic iron that could be included in the steel flow chart of the electric or basic oxygen furnace.

Midrex and HYL (direct gas–solid reduction process, developed by the Mexican company HYLSA)<sup>[2]</sup> processes represent the entire world production of sponge iron (DRI, direct reduction iron). There are also a number of alternatives for producing DRI that have not passed the semi-industrial scale.<sup>[3–5]</sup> Recently we apply an interesting kind of DRI process, using a fluid bed furnace designed by CENIM and installed at the Almeria Solar Platform (PSA-CIEMAT). This furnace uses fluidized bed technology, in

[\*] I. Ruiz-Bustanza, J. Mochón, F. Garcia-Carcedo, A. J. Vázquez  
Centro Nacional de Investigaciones Metalúrgicas (CENIM-CSIC),  
Avda. Gregorio del Amo, 8, 28040 Madrid, Spain  
Email: irbustanza@cenim.csic.es  
I. Cañadas, J. Rodríguez  
PSA-CIEMAT, Plataforma Solar de Almería, CIEMAT, P.O. Box 22,  
04200 Tabernas (Almería), Spain  
L. Felipe Verdeja  
Group of Investigation in the Iron and Steel Industries,  
Metallurgy and Materials, School of Mines, University of Oviedo,  
C/Independencia 13, 33004 Oviedo (Spain) Associated Unit to  
CENIM-CSIC, Spain

Element	Composition [%]
FeO	75
Fe <sub>2</sub> O <sub>3</sub>	5
Fe	10
Other	10

**Table 1.** Chemical analysis – elementary “mill scale.”

which the material to be treated is suspended in a fluid gas with a N<sub>2</sub>–5% H<sub>2</sub> reducing agent,<sup>[2,3,6]</sup> but bed heating comes from concentrated solar energy (CSE) with no fossil fuel consumption nor CO<sub>2</sub> production.

Most of renewables energies, e.g., wind, photovoltaic, are directly connected with the transformation of mechanical energy to electricity production. Solar thermal electricity is produced by heating air at high temperatures to generate the steam and finally electricity in the conventional way. This solar energy application allows direct utilization of the high temperature air/gases obtained to different chemical and metallurgical processes without the intermediate step of electricity production. This direct utilization of heated gases in processes, avoiding all steps of 1 – electricity production, 2 – high voltage transformation, 3 – transmission, 4 – low voltage transformation, and 5 – final heating application in process, allows an increment in total solar energy yield.

All metallurgical and chemical processes have intermediate steps where heating and cooling of materials to be processed is needed. In those processes, it is possible to use High Temperature Solar Thermal Energy for fluid heating as a vector for heating those materials.

This paper is in the line of the actual general interest to study the potential uses of solar heat in industrial processes showing a specific direct industrial application. Vannoni et al.<sup>[7]</sup> analyzes the temperature level of different industrial processes in different industrial sectors and concludes that more than 90% of non-metallic materials (ceramic) and basic metals are sectors where process temperature is over 400°C.

We show the application possibility of CSE in a medium-high temperature chemical-metallurgical process. Here the highest saving in energy use is more profitable than that in low mean temperature industrial processes. However the reported for the operating capacity of solar thermal plants in industry is very small, only 0.02%, 25 MW<sub>th</sub> versus 118 GW<sub>th</sub> (168 Mm<sup>2</sup>). Vannoni says this comparison is not strictly correct from a methodological point of view because 25 MW<sub>th</sub> is the output of a collection of built examples in 21 countries and not a systematic review of the installed plants for industrial processes.

Even though the difference between both figures is enough relevant and the potential of using a solar thermal for providing heat to industrial application is really relevant. **Figure 1** shows the distribution by industry sector of solar industrial process heat plants.<sup>[8]</sup> We must point out that ceramic and metal industries, whose processes are made at higher temperatures, are not included; there is only a mention to Chemistry where they are usually not included. All other industries are characterized for their low mean process temperature. **Figure 2** shows the distribution by country.

It is clear that most and easier applications are those concerned with domestic heating and cooling and hotel hospital and similar applications because of their higher number of possible applications, but it is a matter of fact that industry is the higher energy consumer. But there is a strong “mental curtain.” The success of this low temperature applications hidden the tremendous possible energy saving in ceramic, metallurgic, and chemical industries. We devote our work to demonstrate that different metallurgical materials processing can be made with CSE<sup>[9]</sup> to try to cut this curtain. This paper is another show that it is possible.

## 2. Metallurgical Wastes

Although this paper is not intended to be exhaustive in addressing this problem, we would at least like to lay out which applications, in our opinion, are of highest priority when considering the introduction of solar thermal energy

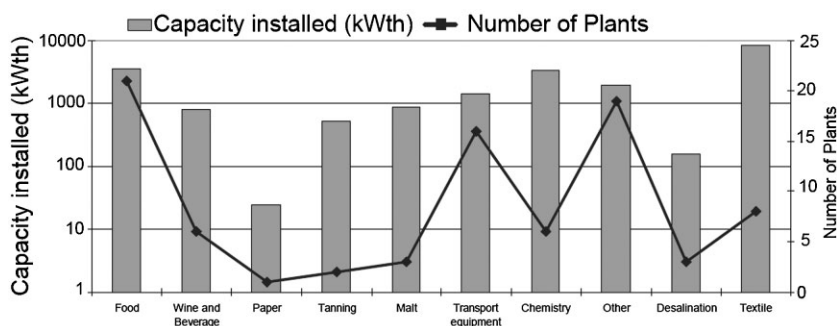


**Figure 1.** Solar industrial process heat plants – distribution by industry sector – October 2007.

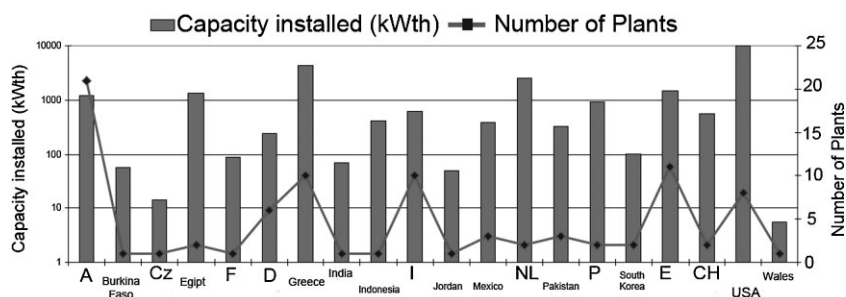


Figure 2. Solar industrial process heat plants – distribution by country – October 2007.

to metallurgical waste recycling. The three main objectives of CSE application in the fluid bed heating process are:

1. Independence of fossil fuel supply,
2. Utilization of own natural resources, and
3. Reduction in CO<sub>2</sub> production in high temperature industrial processes.

In Table 2–4 are detailed the most characteristic chemical properties of the most representative steel waste products. While for some of them, particularly for blast furnace slag, generated on the order of 300 kg of slag per ton of pig iron (Table 2), the problem of its use in civil engineering is well documented,<sup>[10–12]</sup> for the vast majority of the remaining waste there is still no completely satisfactory solution.<sup>[2,13]</sup>

After blast furnace slag, the second most important residue, due to the amount produced, around 125 kg slag per ton of steel manufactured in the LD converter (initials of Austrian cities of Linz and Donawitz where the process was developed in 1952), is the BOF conversion slag (Basic Oxygen Furnace), as see in Table 2.

The main drawbacks of these types of slag are in their chemical/physical instability (free CaO is present, not combined with any acidic oxide). The chemical character-

istics of electric furnace slag in the manufacture of carbon steels are similar to the BOF in Table 2 as long as they increase the level of FeO in the table, and decrease the CaO by 15%.

The electric furnace slag directed from the production of stainless steel and high alloy steels is different, due to the quantities, in the vicinity of 1% for chromium oxide, nickel, vanadium, molybdenum or titanium, which can be found.

Among the four steel waste products considered, there are the dust from the blast furnace (dry purification) and the blast furnace sludge (wet scrubber), with compositions shown in Table 3. And finally in Table 4, there are compositions for LD converter dust produced in BOF steel-making and the electric furnace dust (EAF). While flying debris of LD are characterized by high ratios of FeO, those corresponding to the blast furnace are identified by high proportions of redoubts. Finally, the waste carried by electric furnace gases is characterized by high zinc content.<sup>[14,15]</sup>

Obtaining 100% magnetite is feasible by performing process in the solar oven, which allows obtaining a byproduct

Composition	BF slag [%]	BOF slag [%]
CaO	40–46	42–50
SiO <sub>2</sub>	31–38	10–13
Al <sub>2</sub> O <sub>3</sub>	10–16	1–3
MgO	5–10	1–8
MnO	1–3	3–7
FeO	<1	15–25
Fe <sub>2</sub> O <sub>3</sub>		1–5
P <sub>2</sub> O <sub>5</sub>		1–4
Others (<1%)	TiO <sub>2</sub> , K <sub>2</sub> O, Na <sub>2</sub> O, S, P	

Table 2. Blast furnace and LD (BOF) slags.

Composition	Dust from the BF (dry scrubber) [%]	BF sludge (Wet scrubber) [%]
CaO	6.60	6.50
SiO <sub>2</sub>	22.5	18.5
Al <sub>2</sub> O <sub>3</sub>	0.70	1.50
MgO	0.50	1.50
MnO	0.20	0.80
FeO	2.50	5.20
Fe <sub>2</sub> O <sub>3</sub>	9.50	38.00
C	42.50	2.20
H <sub>2</sub> O	15	25
Zn + Pb		0.80

Table 3. Dust from the BF (dry scrubber) and Blast furnace sludge (wet scrubber).

Composition	LD converter dust (BOF) [%]	EAF [%]
CaO	17.10	4–5
SiO <sub>2</sub>	0.82	5–7
Cr <sub>2</sub> O <sub>3</sub>		0.1–3.5
MgO	8.30	1.5–3.5
MnO	2.40	1–2.5
FeO	35.72	15–36
Fe <sub>2</sub> O <sub>3</sub>	30.50	1–3.5
C	1.70	1.3–1.7
ZnO		14–40
PbO		1–3.5
Others	3.18	1–3.5

**Table 4.** LD converter dust (BOF) and electric furnace dust (EAF).

with special magnetic properties susceptible of concentration by traditional methods, commonly used to produce concentrates from raw materials by magnetic separation.

Solar energy would be a step to recycle products, with high concentrations of Fe<sub>3</sub>O<sub>4</sub> and free from harmful contaminants, which can be added to the steelmaking process to make a high quality steel.

Specifically, using the solar furnace plant of Almería (Spain), the process has been tested with the mill scale, one of the less complex metallurgical wastes from the chemical point of view (Table 1). We have tried to demonstrate the possibility of reach an experimental certainty about the following issues:

- The possibility of using the solar furnace for the partial reduction of Fe<sub>2</sub>O<sub>3</sub> to Fe<sub>3</sub>O<sub>4</sub>.
- Obtaining a of high purity Fe<sub>3</sub>O<sub>4</sub> product, commonly used as feedstock for aluminothermy welding of railway rails.

The fact that achieve the above objectives, treating mill scale, has led the authors to extrapolate these results to other applications of solar energy in the other residues mentioned above; dust and sludge from the blast furnace, the LD converter dust and the EAF, and also to other raw materials such as sintered product that currently feeds most of the blast furnaces in integrated steel production of carbon steels.

From the experimental data obtained from the treatment of mill scale, the following applications of solar energy could be considered:

- Convert the iron ore fines used in the sintering process, mostly Fe<sub>2</sub>O<sub>3</sub>, to magnetite (Fe<sub>3</sub>O<sub>4</sub>).

- The possibility of heating the sinter (or pellet) that feed the furnaces.
- Partial reduction of the sintered or pelletized iron burden that feeds the BF.
- Reduction of the sintering powders, which have high contents of alkalis, halogen, and sulfur, to form magnetite and with subsequent magnetic separation to release magnetite from the non-ferrous contaminants previously indicated.

### 3. Experimental Results: The Reduction of Hematite to Magnetite in a Solar Furnace

The equipment used to perform the transformation of Fe<sub>2</sub>O<sub>3</sub> (hematite) to Fe<sub>3</sub>O<sub>4</sub> (magnetite), consists of a fluidized bed furnace heated with the CSE from the horizontal axis solar furnace installed in the Almeria Solar Platform (PSA-CIEMAT).

The basic elements of the solar furnace are: a heliostat with a 120 m<sup>2</sup> reflective surface that follow the sun way and redirects the reflected beams to a multifaceted parabolic concentrator mirror, an attenuator or shutter, a 90.5 m<sup>2</sup> multifaceted parabolic concentrator mirror with 89 facets, a honeycomb SiC absorber, a fluidized bed and an air cleaner. In Figure 3, two views of the installation can be seen:<sup>[16,17]</sup> (Figure 3a) heliostat and front building with attenuator, and (Figure 3b) multifaceted parabolic concentrator on the left side, and honeycomb absorber on the right side. A circular parabolic concentrator can be seen in the back but it is out of this work.

Every morning when the installation is connected, the heliostat faces the sun and follows the sun's movement and directs reflecting sun beams, through the attenuator, situated on the front wall of the building, to the multifaceted parabolic mirror situated on the back wall of the building. The attenuator, or shutter, can rotate each horizontal piece to control incident power flux (Figure 4).

Concentrated beams by the multifaceted parabolic mirror strike the absorber and heat the surface of the honeycomb material, SiC. Temperatures as high as 1100°C can be achieved. The “honeycomb” form of the SiC absorber consists of a series of holes on a square base with very thin walls, located in front of the fluidized bed furnace. This design increases the heated surface of the absorber to enhance the heat transference to the air flowing through the holes. A vacuum pump at the end of the installation forces air through the absorber; the air is heated up to 900–1000°C.

The fluid bed furnace (Figure 5) is a double-tube: the inner tube contains the fluidizing mass which is indirectly heated through the wall by the hot air which comes from the absorber flowing by the crown between the two tubes. The exit air, still warm, is then used to preheat the fluidizing air or gas that is fed through a helicoidal tube in the preheater. This preheated fluidizing air or gas of controlled

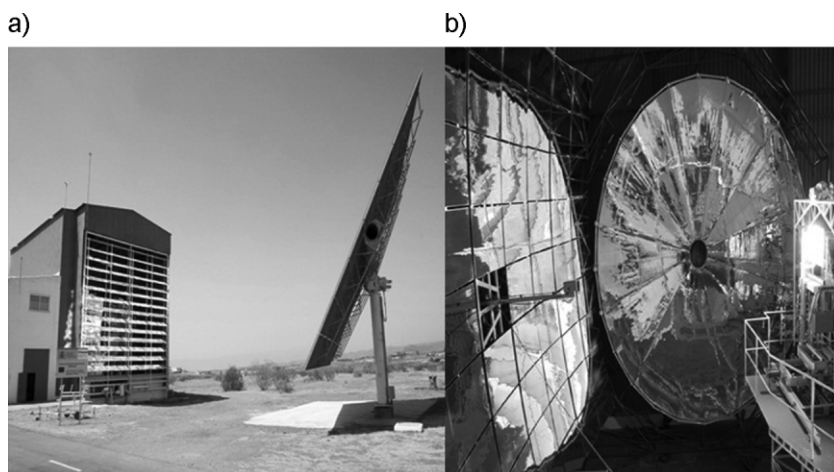


**Figure 3.** a) Heliostat (right) and frontal view of the attenuator on the building where solar furnace is located. b) Multifaceted parabolic concentrator (left) and absorber at the bed entrance (right).

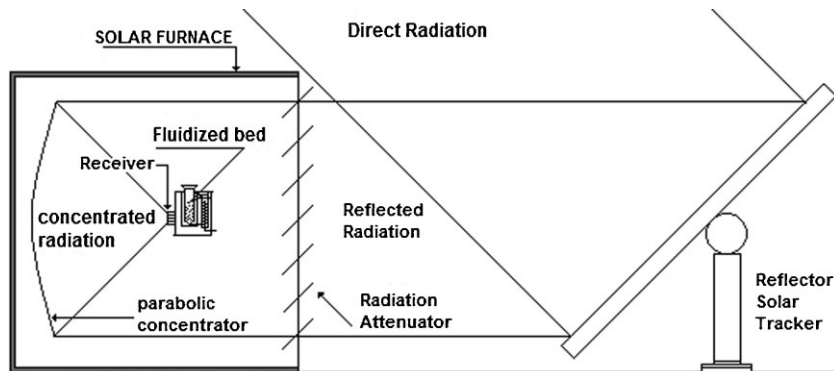


**Figure 4.** Basic layout of solar concentrator and fluidized bed.

composition is introduced into the inner tube of the fluidized bed, where the particles are fluidized, through a conical entrance closed by a ball.

This design is considered much better than other Concentrated Solar heated fluidized beds cited in the literature,<sup>[18]</sup> in which the heating takes place either on the top of the bed or through a quartz window on one side.

The independence of the two gases, the heating air outside the inner fluidized bed tube in the annular zone and the fluidizing gas preheated by it, allows us to work not only with gases of different compositions but also with independent control of flow rates. Also an independent temperature control can be made by a second electric preheating of the gas fluidizing tube just before the gas to come into the fluidizing bed.

The fluidization gas used in this work was nitrogen with 5% hydrogen. The control of the operation was made on the fluidization gas flow and the temperature, along with the size of the attenuator opening, was recorded in the bed. Due to the characteristics of the bubbling fluidized bed furnace, the size of the particles to be treated must

be as homogeneous as possible to avoid pulling in the gases emerging from the top.<sup>[19]</sup> Therefore, the mill scale is previously agglomerated on a pelletizing disc of 1.5 m diameter at CENIM.

Subsequently, the pelletized material was treated (oxidized)-stabilized in a furnace until it was completely converted to hematite,  $\text{Fe}_2\text{O}_3$ . The X-ray diffraction confirms that the final product obtained is 100% hematite.

The reduction tests were conducted with hematite pellets introduced into the fluidized bed furnace which was heated to a temperature of  $750^\circ\text{C}$  for 40 min.

**Figure 6** shows curves of sudden sunshine (curve 1), to the opening of the shutter control valve, (curve 2), to the applied power (curve 3), and the bed temperature (curve 4). Applied power density and temperature are shown at left ordinate and opening percentage at right ordinate.

It can be seen that a decrease in irradiation due to the closing of shutter, equivalent to the passage of a cloud overhead (curve 2), which lasted several minutes, has minimal influence on the temperature of the fluidizing bed (curve 4).

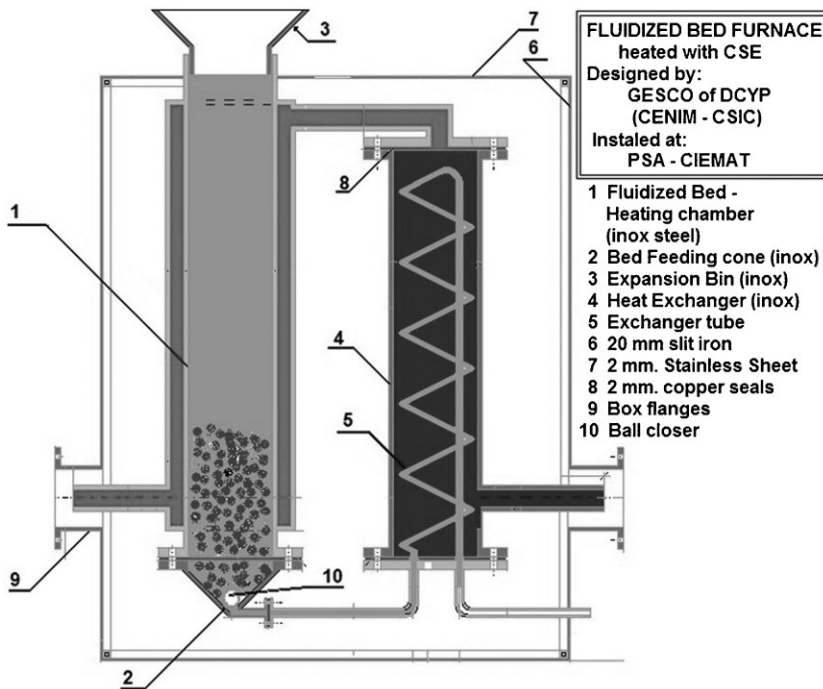


Figure 5. Fluidized bed scheme.

The reason for this fairly good maintenance in temperature is that hematite has high specific heat and thus acts as a heat accumulator. This high temperature stability of the fluidized bed reveals its suitability as a reactor for use in solar energy testing even if fluctuations in irradiance occur.

In any case, to prevent a temperature drop due to low insolation during the longest heating times, it is recommended that the bed has a parallel heating system using gas or electricity, to prevent any possible drops in temperature from occurring in the furnace. This fluid bed furnace,

with the parallel heating system, allows an uninterrupted annual operating time in which the use of solar thermal energy will produce energy savings.

These savings will be highest for a single work day, coinciding with the peak hours of solar irradiance, and lower in the case of two or more shifts. However, solar thermal energy can be stored in fluids (liquid metals and molten salts) with high heat storage capacity, which can then be recovered during the night hours or during periods of low insolation.<sup>[20]</sup> In the case of this type of facility,

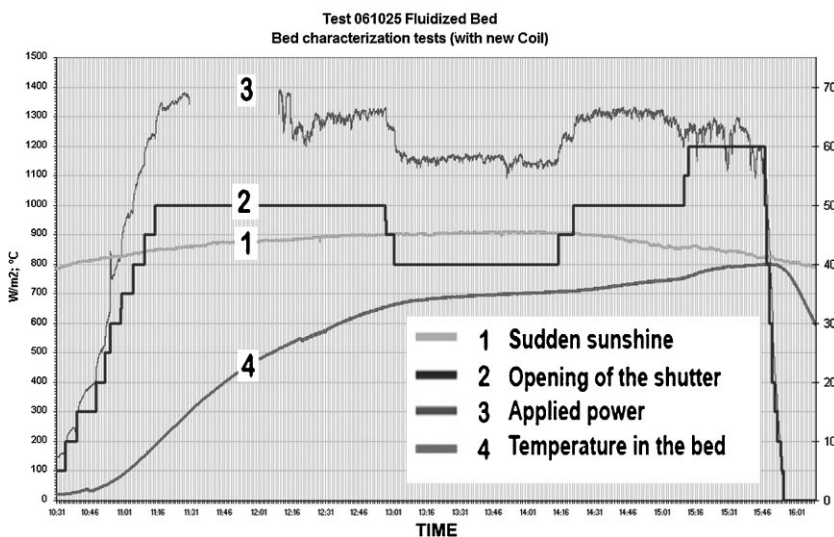


Figure 6. Diagram of bed operation.

which requires a large investment, it is preferable that all energy consumed is of solar origin.

From X-ray diffraction analysis of the product after the treatment (Figure 7), we can see that the performance of the reduction has been 100%. This could be seen in a simple visual comparison of the reddish color of the initial hematite on the fluidized bed with the black final result (Figure 8). In this way, additionally, we saw that all the magnetite was separated by a magnet.

## 4. Results and Discussion

In order to support the conceptual aspects of thermodynamics and kinetics arising from the application of solar

thermal systems Fe—O—C and Fe—O—H, the following points need to be considered:

- The possible phases in equilibrium can be achieved between the different compounds of iron and reducing agent/oxidizing gas.
- The kinetic mechanisms that can be used in the treatment of the different compounds of the Fe—O system in solar reactor furnaces. If mill scale was in a rotary kiln or hearth.

If the mill scale was produced in an open-air atmosphere without forced air recirculation at a temperature of 900°C, the product obtained would be a mixture of magnetite, Fe<sub>3</sub>O<sub>4</sub> (66%) and hematite, Fe<sub>2</sub>O<sub>3</sub> (34%). The reducing potential initially present in the system at the

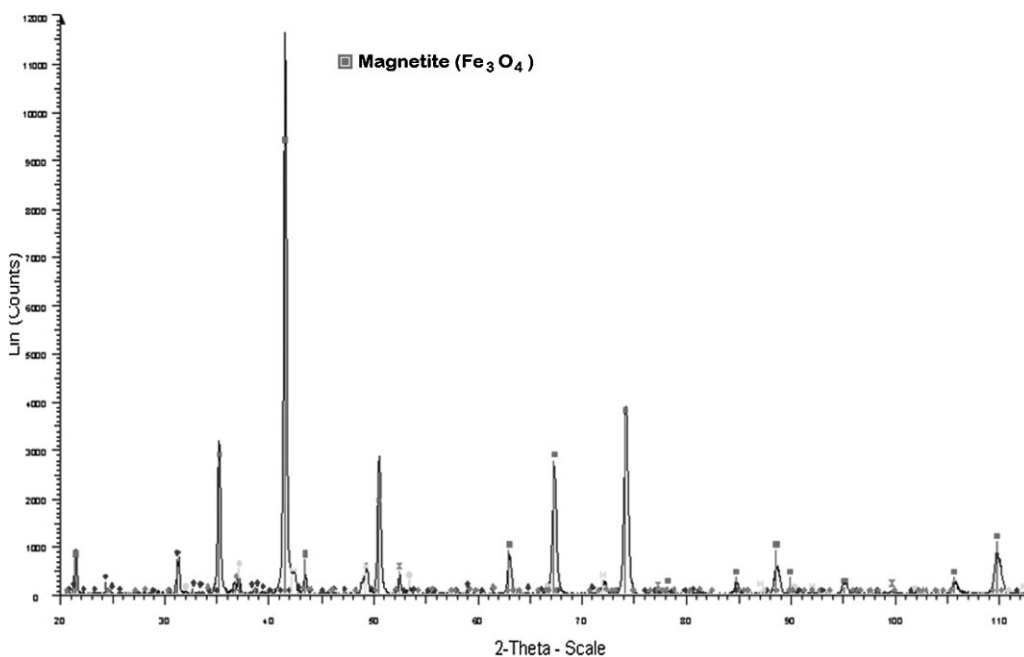


Figure 7. X-ray diffraction of obtained magnetite.

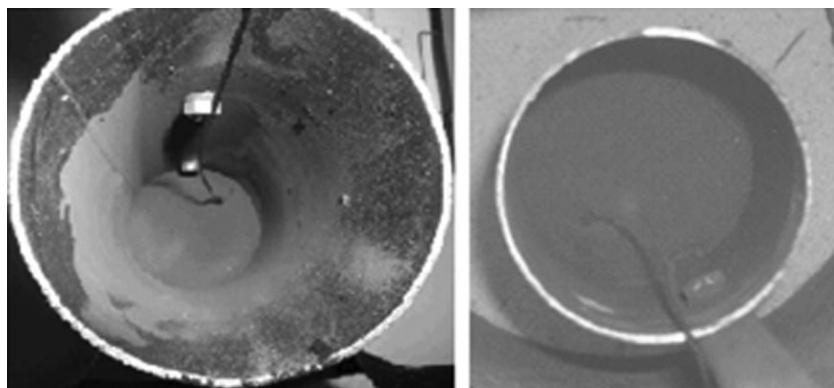


Figure 8. Views of the fluidized bed from above. Left: hematite; right: magnetite.

beginning of the operation (oil mill) is offset by the oxidizing environment, which promotes the formation of  $\text{Fe}_2\text{O}_3$  at the end of the treatment. It is this slightly reducing atmosphere at the start of the treatment which results in a less than complete oxidation of FeO and allows for the production of a substantial amount of hematite, whose characteristic red color can be seen in the diagram in Figure 9.<sup>[2]</sup>

Finally, the generation of magnetite,  $\text{Fe}_3\text{O}_4$ , from hematite,  $\text{Fe}_2\text{O}_3$ , in the solar fluid bed furnace in an atmosphere of 5%  $\text{H}_2$  is thermodynamically compatible with the predictions illustrated in Figure 10 for the Fe—H—O system.<sup>[2]</sup>

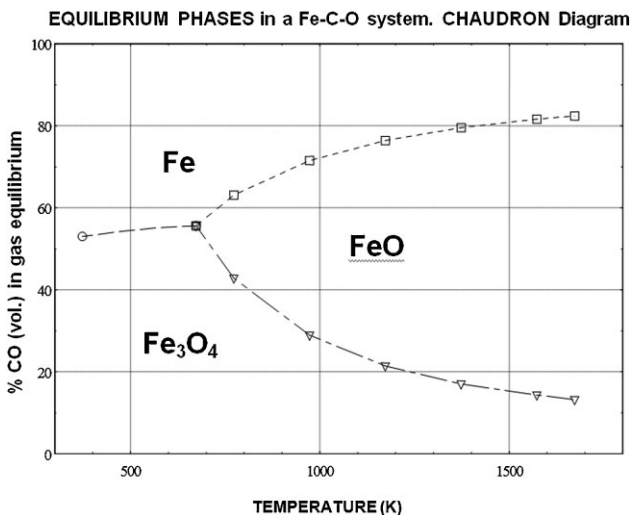


Figure 9. Equilibrium phases in a Fe—C—O system, as a function of temperature and volumetric composition of CO in the gas for any total system pressure value.

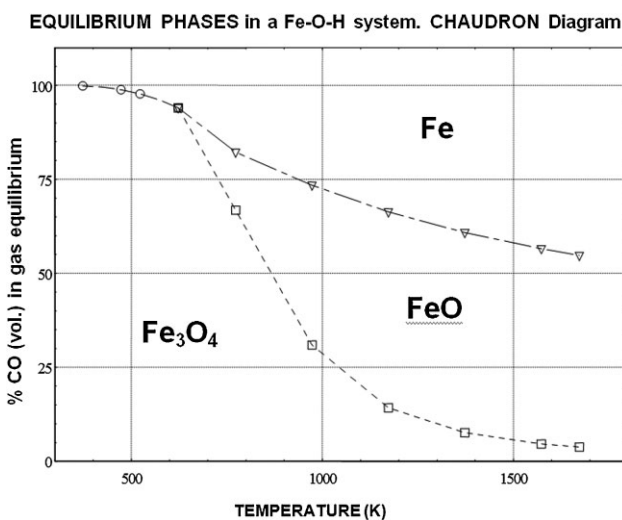
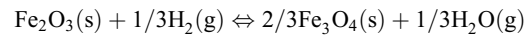


Figure 10. Equilibrium Phases in a Fe—H—O system, as a function of temperature and volumetric composition of CO in the gas for any total system pressure value.

From the energy standpoint, standard enthalpy ( $\Delta H^0$ ) associated with the reaction:



Is slightly endothermic and does not vary substantially with temperature. A constant value independent of the operating temperature of the solar furnace equal to  $19.22 \text{ kJ t}_{\text{Fe}_2\text{O}_3}^{-1}$  can be assigned.<sup>[2]</sup>

Kinetic considerations of the reduction of hematite to magnetite are based on the diffusional control of the gas through the oxide layer reaction product (magnetite,  $\text{Fe}_3\text{O}_4$ ).

To measure the extent of the reaction, a non-dimensional parameter  $X$ , can be used, defined in the following equation:

$$X = \frac{V_o - V_i}{V_o} \quad (1)$$

where  $V_o$  is the volume of the particulate material at time zero, before the reaction begins, while  $V_i$  is the particulate volume which has not reacted after a determined period of time,  $t$ . Clearly, when the reaction is completed,  $V_i = 0$ , and  $X = 1$ . The kinetic equation would be:<sup>[2,17]</sup>

$$1 - \frac{2}{3}X - (1 - X)^{2/3} = kt \quad (2)$$

where the kinetic constant of this “topochemical process” is equal to:

$$k = \frac{D_{i-e}C_0}{\rho_g r_0^2} \quad (3)$$

With  $D_{i-e}$  being the effective gas diffusion coefficient through the open porosity of the reaction product. That is:

$$D_{i-e} = \frac{D_{\text{H}_2} p_a}{\sqrt{2}} \quad (4)$$

where  $D_{\text{H}_2}$  is the hydrogen diffusion coefficient in the gas and  $p_a$  is the open porosity of the material per unit. The rest of the variables involved in the rate constant of this “topochemical reaction” are:  $C_o$ , the concentration of reducing gas ( $\text{H}_2$ ).  $\rho_g$  and  $r_o$ , which are, respectively, the overall density or mass and the radius of the hematite pellets.

The times required for the complete conversion (reduction) of hematite,  $\text{Fe}_2\text{O}_3$ , to magnetite,  $\text{Fe}_3\text{O}_4$ , for different temperatures are shown in Table 5:  $X=1$ , in the kinetic Equation 1.<sup>[21]</sup> As can be seen, the times shown in Table 5 agree with the experimental data obtained in the solar furnace.

Given that the sinter obtained from iron raw materials with high percentages of magnetite and that the consumption of coke decreases significantly with respect to the agglomeration of hematite, the solar furnace could be a

Total reduction time [minutes]	Temperature [°C]	Temperature [K]	$K$ [ $\text{min}^{-1}$ ]
40.5	400	673	8.227E-03
31.6	500	773	1.056E-02
25.4	600	873	1.314E-02
20.9	700	973	1.597E-02
17.5	800	1073	1.905E-02

**Table 5.** Kinetic parameters associated with solid–gas reduction in the Fe–H–O system.

tool used to reduce coke rates (the consumption of coke) in mixtures of iron raw materials that need to be sintered.

Thirty percent of  $\text{Fe}_3\text{O}_4$  in the iron to be sintered decreases the amount of coke required to achieve a high

performance product: from 6% of coke in the mix, one can reach as low as 5%,<sup>[22]</sup> a 16% less than coke needed initially.

Finally, through a comparative cost study of the obtaining of 1 t of DRI by two different production methods,<sup>[23]</sup> the first of them using natural gas as a reducing agent and energy source and the second in which the energy source is natural gas and reducing element is coal:

- (a) The traditional Midrex method – in **Table 6**.<sup>[2,3]</sup>
- (b) Various alternative processes to pilot or semi-industrial scale, whose common denominator is the use of non-coking coal as the majority of reducing agent, **Table 7**.<sup>[2,3]</sup>

It can be shown that allowing for the cost of setting up a DRI plant with a solar furnace, and taking into account the savings that would be accrued through the decrease in the cost of energy consumption in such a plant, the alternative proposals considered here would be competitive with regard to the bottom line.

Variable	Specific cost	€ t <sup>-1</sup> of DRI
Natural gas [10.5 GJ t <sup>-1</sup> DRI]	4.5 € GJ <sup>-1</sup> (2.25 € GJ <sup>-1</sup> )	47.25 € (23.63 €)
Electricity [120 kWh t <sup>-1</sup> DRI]	0.12 € kWh <sup>-1</sup> (0.055 € kWh <sup>-1</sup> )	14.40 € (6.60 €)
Manpower + Administration [0.20 man-hour t <sup>-1</sup> DRI]	30 € man-hour <sup>-1</sup>	6.0 €
H <sub>2</sub> O [1.5 m <sup>3</sup> t <sup>-1</sup> DRI]	1.50 € m <sup>-3</sup>	2.25 €
Maintenance [4 € t DRI]	–	4.0 €
Iron charge [1.50 t t <sup>-1</sup> DRI]	30 € t <sup>-1</sup>	45 €
Amortization [10 year-5.0 × 10 <sup>5</sup> t DRI year]	130 € t <sup>-1</sup> DRI-year	13.0 €
Total	–	131.9 € (100.48 €)

**Table 6.** Midrex Process Prices (per ton of DRI) Year 2010.

Variable	Specific cost	€ t <sup>-1</sup> de DRI
Natural gas [3.0 GJ t <sup>-1</sup> DRI]	4.5 € GJ <sup>-1</sup> (2.25 € GJ <sup>-1</sup> )	13.50 € (6.75 €)
Electricity [135 kWh t <sup>-1</sup> DRI]	0.12 € kWh <sup>-1</sup> (0.055 € kWh <sup>-1</sup> )	16.20 € (7.43 €)
Manpower + Administration [0.30 man-hour t <sup>-1</sup> DRI]	30 € man-hour <sup>-1</sup>	9 €
H <sub>2</sub> O [1.3 m <sup>3</sup> t <sup>-1</sup> DRI]	1.50 € m <sup>-3</sup>	1.95 €
Maintenance [5.0 € t <sup>-1</sup> DRI]	–	5 €
Iron charge [1.30 t t <sup>-1</sup> DRI]	30 € t <sup>-1</sup>	39 €
Reducer (Coal) [0.38 t t <sup>-1</sup> DRI]	100 € t <sup>-1</sup>	38 €
Amortization [10 year-5.0 × 10 <sup>5</sup> t DRI-year]	140 € t <sup>-1</sup> DRI-year	14 €
Total	–	136.65 € (121.13 €)

**Table 7.** Fastmet-Inmetco-Comet Prices (per ton of DRI) – Year 2010.

Obviously, when treating ferrous-carbon waste in a solar furnace, not only would there be a cost savings derived from using less energy and requiring less iron ore in the first place, but also those related to reducing consumption (by recycling waste, which would save a lot of carbon).

In this case, the profit and cost savings that would result from the installation of a solar furnace, despite the initial investment associated with it, would be greater.

## 5. Conclusions

This paper shows how a fluidized bed heated by solar energy reduces pelletized hematite to magnetite. The temperatures reached in the bed are far superior to the minimum necessary to achieve the reduction of hematite with hydrogen (a mixture of 5% hydrogen in nitrogen).

We can conclude:

1. Concentrated solar energy (CSE) is a suitable way to heat a fluidized bed at high temperatures. CSE heated fluid bed is a reactor suitable to perform reduction of mill scale and many other reactions using this kind of reactor at reaction temperatures up to those obtained in this work.
2. Intermittence of solar irradiance, simulated with a closing of shutter, don't produce variations that affect the heating process of the fluid bed thanks to the thermal inertia of reactants inside the bed. Secondary electric heating was not needed in this work to compensate possible insufficient heating due to variations in sun irradiance.
3. The industrial reduction of hematite to magnetite can be performed with CSE. If we would like to work  $24 \text{ h day}^{-1}$  we need to introduce parallel heating systems (electric or gas) or introduce existing fluid storage systems for high use of CSE.
4. The system of preheating fluidizing gas may be improved upon using a helicoidal tube in a second bed with sand, which would fluidize with hot air, instead of the current design.
5. With the practice of double heating, energy conservation in addition to a reduction in  $\text{CO}_2$  emissions is evident, on an annual basis, if a  $\text{N}_2/\text{H}_2$  mixture is used as a reducing agent. The estimated production of  $\text{CO}_2$ , now, in a reasonably sunny location, is on the order of 70/80% of energy consumption, which might be higher if the processing temperature were lower.
6. The use of solar furnaces must be introduced to all kind of processes chemical or metallurgical and, certainly, in those of recycling when medium or high temperatures are needed as it happens in the treatment of any steel waste as noted in this project (including those considered "eco-toxic"). Even in conventional processes CSE can be used for preheating of combustion air with independence of the temperature obtained according

the kind of concentrator equipment. In all of them savings in energy costs and raw materials (ferrous and reducers), may provide some leeway in assessing the investment needed to install solar DRI-reduction facilities, compared to the existing DRI plants in the market.

7. It has been shown that it is possible to carry out the reduction of hematite to magnetite in a solar furnace, from a steel by-product like the mill scale. It could think about apply this knowledge to other areas of the steel-making process, as in the partial reduction of iron ores used in the burden of sinter process.

## Acknowledgments

This work was performed under the PSA-CENIM agreement within the CIEMAT-PSA framework for joint use of facilities. The authors wish to thank Mr. Javier Llorente for his help during the research.

Received: June 6, 2012;

Published online: October 12, 2012

**Keywords:** mill scale; steel by-products; concentrated solar energy; fluidized bed furnace

## References

- [1] A. I. Babich, H. W. Gudenau, K. T. Mavrommatis, C. Froehling, A. Formoso, A. Cores, L. Garcia, *Rev. Met. Madrid* **2003**, 39, 288.
- [2] J. P. Sancho, L. F. Verdeja, A. Ballester, *Metalurgia Extractiva: Procesos de Obtención*, Ed: Síntesis, Madrid, **2000**, p. 45.
- [3] A. Conejo, *Rev. Met. Madrid* **2000**, 36, 420.
- [4] H. W. Gudenau, European Commission. Technical Steel Research EUR 18637 DE, **1998**, 165.
- [5] R. Steffen, K. Tacke, W. Pluschkell, European Commission. Technical Steel Research EUR 18559 DE, **1998**, 321.
- [6] M. Hirsch, A. Hollnagel, A. Orth, European Commission. Technical Steel Research EUR 18772 DE, **1999**, 322.
- [7] C. Vannoni, R. Battisti, S. Digo, *Potential for Solar Heat in Industrial Processes*, Ed: CIEMAT, Madrid, IEA SHC Task 33 and Solar PACES Task IV: Solar Heat for Industrial Processes **2008**, p. 18.
- [8] G. C. Vannoni, R. Battisti, S. Digo, *Potential for Solar Heat in Industrial Processes*, IEA SHC and Solar PACES Ed: University of Rome, Rome **2008**, p. 21.
- [9] A. J. Vázquez, *La Energía Solar Térmica Directa: Una Opción Ignorada por la Industria*, Proc. Congress Cies 2012, Vigo **2012**, p. 203.
- [10] V. A. Mymrin, A. J. Vázquez, *Steel World* **2000**, 5, 33.
- [11] V. A. Mymrin, A. J. Vázquez, *Miner. Eng.* **1999**, 12, 1399.

- [12] V. A. Mymrin, A. J. Vázquez, *Waste Manage. Res.* **2001**, *19*, 465.
- [13] A. Babich, D. Senk, H. W. Gudenau, T. T. Mavrommatis, *Ironmaking*, Ed: RWTH Aachen University, Department of Ferrous Metallurgy, Aachen, Germany, **2008**, p. 228.
- [14] R. Fisher, M. W. Briggs, S. S. Baker, M. I. Pistelli, G. Harp, J. Pereira-Gomes, European Commission, Technical Steel Research, EUR 21432 EN, **2005**, 154.
- [15] M. Estrela, J. Gomesand, M. Vrhovac, European Commission, Technical Steel Research, EUR 18419 EN, **1998**, 187.
- [16] P. Rufes, *Energía Solar Térmica: Técnicas de Aprovechamiento*, Ed: Marcombo, Barcelona, **2010**, p. 67.
- [17] I. Cañadas, D. Martínez, J. Rodríguez, B. J. Fernández-González, A. J. Vázquez, *Procesamiento en Lechos Fluidizados Calentados por Energía Solar Concentrada*, Ed: CIES, Santiago de Cuba, **2006**, p. 66.
- [18] R. Koenisdorff, P. Kienzle, *Solar Energy Mater.* **1991**, *24*, 279.
- [19] A. Ballester, L. F. Verdeja, J. P. Sancho, *Metalurgia Extractiva: Fundamentos*, Ed: Síntesis, Madrid, **2000**, p. 188.
- [20] T. Nomura, N. Okinawa, T. Akiyama, *ISIJ Int.* **2010**, *50*, 1229.
- [21] H. Mookherjee, H. S. Ray, A. Mukherjee, *Ironmaking Steelmaking* **1986**, *13*, 229.
- [22] P. R. Dawson, *Ironmaking Steelmaking* **1993**, *20*, 135.
- [23] L. F. Verdeja, A. Alfonso, M. F. Barbés, C. Goñi, *Proc. Jornadas Siderurgia Aceralia*, University of Oviedo, **2004**, 45.